

Low-dimensional paradigms for high-dimensional hetero-chaos

Yoshitaka Saiki, Miguel A. F. Sanjuán, and James A. Yorke

Citation: *Chaos* **28**, 103110 (2018); doi: 10.1063/1.5045693

View online: <https://doi.org/10.1063/1.5045693>

View Table of Contents: <http://aip.scitation.org/toc/cha/28/10>

Published by the [American Institute of Physics](#)

Articles you may be interested in

[Quasiperiodic perturbations of heteroclinic attractor networks](#)

Chaos: An Interdisciplinary Journal of Nonlinear Science **28**, 103111 (2018); 10.1063/1.5050081

[A general framework for boundary equilibrium bifurcations of Filippov systems](#)

Chaos: An Interdisciplinary Journal of Nonlinear Science **28**, 103114 (2018); 10.1063/1.5037947

[Collective mode reductions for populations of coupled noisy oscillators](#)

Chaos: An Interdisciplinary Journal of Nonlinear Science **28**, 101101 (2018); 10.1063/1.5053576

[Two-dimensional spatiotemporal complexity in dual-delayed nonlinear feedback systems: Chimeras and dissipative solitons](#)

Chaos: An Interdisciplinary Journal of Nonlinear Science **28**, 103106 (2018); 10.1063/1.5043391

[Stability and predictability in human control of complex objects](#)

Chaos: An Interdisciplinary Journal of Nonlinear Science **28**, 103103 (2018); 10.1063/1.5042090

[Testing dynamical system variables for reconstruction](#)

Chaos: An Interdisciplinary Journal of Nonlinear Science **28**, 103117 (2018); 10.1063/1.5049903



Don't let your writing
keep you from getting
published!

AIP | Author Services

Learn more today!

Low-dimensional paradigms for high-dimensional hetero-chaos

Yoshitaka Saiki,^{1,2,3} Miguel A. F. Sanjuán,^{3,4} and James A. Yorke^{3,5}

¹Graduate School of Business Administration, Hitotsubashi University, Tokyo 186-8601, Japan

²JST, PRESTO, Saitama 332-0012, Japan

³Institute for Physical Science and Technology, University of Maryland, College Park, Maryland 20742, USA

⁴Nonlinear Dynamics, Chaos and Complex Systems Group, Departamento de Física, Universidad Rey Juan Carlos, Tulipán s/n, 28933 Móstoles (Madrid), Spain

⁵Departments of Mathematics and Physics, University of Maryland, College Park, Maryland 20742, USA

(Received 22 June 2018; accepted 26 September 2018; published online 18 October 2018)

The dynamics on a chaotic attractor can be quite heterogeneous, being much more unstable in some regions than others. Some regions of a chaotic attractor can be expanding in more dimensions than other regions. Imagine a situation where two such regions and each contains trajectories that stay in the region for all time—while typical trajectories wander throughout the attractor. Furthermore, if arbitrarily close to each point of the attractor there are points on periodic orbits that have different unstable dimensions, then we say such an attractor is “hetero-chaotic” (i.e., it has heterogeneous chaos). This is hard to picture but we believe that most physical systems possessing a high-dimensional attractor are of this type. We have created simplified models with that behavior to give insight into real high-dimensional phenomena. *Published by AIP Publishing.* <https://doi.org/10.1063/1.5045693>

Prediction and simulation for chaotic systems occur throughout science. Predictability is more difficult when the “chaotic attractor” is heterogeneous, i.e., if different regions of the chaotic attractor are unstable in more directions than in others. More precisely, when arbitrarily close to each point of the attractor there are different periodic points with different unstable dimensions, we say the chaos is heterogeneous and we call it hetero-chaos. In particular, simple illustrative models of hetero-chaotic attractors have been lacking in the literature, and here we present the simplest examples we have found. In fact, our new “baker” maps can be proved to have hetero-chaotic attractors and to be ergodic.

I. INTRODUCTION

Predictability is especially difficult when a trajectory enters a region that has more unstable directions than the region it is leaving. This appears to occur in geomagnetic storms and solar flares¹ or natural hazards² or earthquakes³ or weather.⁴ In such cases, “shadowing” breaks down: numerical simulations no longer reflect true behavior. In our work with simple whole earth weather models (e.g., Ref. 4), the phase space had dimension 3×10^6 , trajectories were chaotic, and we estimate that there were 3×10^4 unstable directions, that is, a tiny ellipse around an initial point would expand in 3×10^4 dimensions. The unstable dimension is usually about one-hundredth of the dimension of the dynamical system. For storm conditions, the regional unstable dimension is higher and thus prediction and simulation and data assimilation are much more difficult.

If the approximate state of the weather is known near some point q in phase space, then after a short time, perhaps a few hours, the possible weather states lie on an expanding

ellipse of some dimension D . We call D the unstable dimension at q . To update the current state of the weather every few hours, it suffices to have enough observations to determine the location of the current state on that ellipsoid. The number of data observations—point measurements of temperature, humidity, pressure, etc. at nearby locations—needed for that is proportional to D which can be far smaller than the dimension of the state space.

For a barotropic atmospheric model, Gritsun^{5,6} found many unstable periodic orbits, and he found a wide variation in their numbers of unstable directions, all coexisting in the same system. He did not attempt to verify that these orbits were in the attractor.

Baker map. Our first examples with hetero-chaos are based in part on the well-known “baker map.” It was defined in 1933 by Seidel.⁷ The map is defined by dividing the square into p equal vertical strips. Seidel used $p = 10$. We use $p = 3$ in Fig. 1, and $p = 2$ is most common in the literature. Each strip is mapped to a horizontal strip by squeezing it vertically by the factor p and stretching it horizontally by the same factor. The resulting horizontal strips are laid out covering the square.

We also show a three dimensional version. In both of these baker maps, the unstable dimension D is 1 and in particular is constant. In such cases, we refer to the chaos as **homogeneous chaos**. The baker maps are area or volume preserving. The earliest use of the map name “baker” that we have found appears in the 1956 *Lectures on Ergodic Theory* by Paul Halmos.⁸ He writes that the actions of the map are reminiscent of kneading dough and that it is “sometimes called the baker’s transformation.”

In the bottom half of Fig. 1, we give a 3D baker map. Here, the unstable dimension is $D = 1$ (and the map contracts the y and z directions). To convert this example into one with unstable dimension $D = 2$ and stable dimension 1, just take

the inverse, mapping each box X' on the right to the box X on the left. For area-contracting (“skinny”) and area-expanding (“fat”) 2D-baker maps, see Refs. 9 and 10, respectively.

Our hetero-chaotic baker maps. The baker maps in Fig. 1 are homogeneously chaotic, but we here modify them to be hetero-chaotic (HC). We introduce two such modified maps in Figs. 2 and 3 as prototypes for understanding attractors with far higher dimension. Our 2D map is not invertible so its relevance to science may seem suspect, but we add one dimension to that map and it becomes our 3D map, which is invertible.

In Fig. 2, there are two regions ($\mathcal{R}_1 = A \cup D$, the left and right thirds of the square) where the dynamics is unstable in one direction (the x coordinate) while in the middle third ($B \cup C$), denoted \mathcal{R}_2 , it is unstable in both x and z coordinates. See Fig. 3 for a 3D invertible volume-preserving version. There exist trajectories that stay in either region but almost every trajectory wanders through the entire square. See Fig. 4 for the homogeneously chaotic invariant set formed by such limited trajectory. We call the set an index set, as described later. For simplicity, we ignore the dynamics of all points on the boundaries of the rectangles A, B, C , and D . In the example, in \mathcal{R}_1 , the map contracts the y direction by a factor of 2 while it expands by a factor of 2 in \mathcal{R}_2 . Hence a periodic orbit

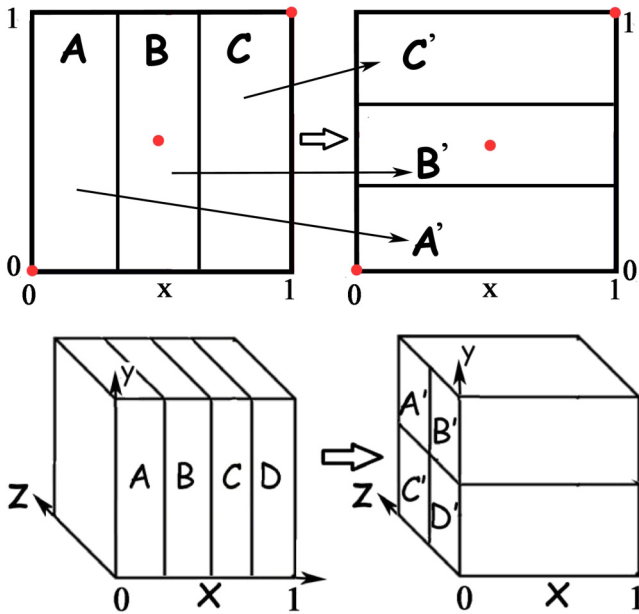


FIG. 1. The homogeneous chaotic baker map in 2D and 3D. Top panel: The standard, i.e., 2D, baker map is defined by splitting the square into p equal-sized vertical slabs where $p = 3$ here. The square is mapped to the square, with $x \mapsto 3x \pmod 1$. Each vertical slab on the left maps to a different horizontal slab on the right, each stretched in the horizontal direction and shrunk vertically. The assignment of which maps to which has been chosen arbitrarily but the assignment is fixed. This map is homogeneously chaotic with one expanding direction. Each slab has a fixed point denoted by a red dot. (Note that two are on slab boundaries). The images are denoted by primes \prime so, for example, A maps onto A' . Bottom panel: We provide a 3D version by slicing a unit cube into four equal-sized pizza-box shaped slabs as shown. The cube is mapped to the cube, using $x \mapsto 4x \pmod 1$ so each pizza-box is expanded to the width of the cube; and each pizza-box maps to a different shoe box-shaped region on the right, each shrunk by a factor of two in the y and z coordinates. The assignment of which pizza-box maps to which shoe box has been chosen arbitrarily but the assignment is fixed. This map is homogeneously chaotic with one expanding direction.

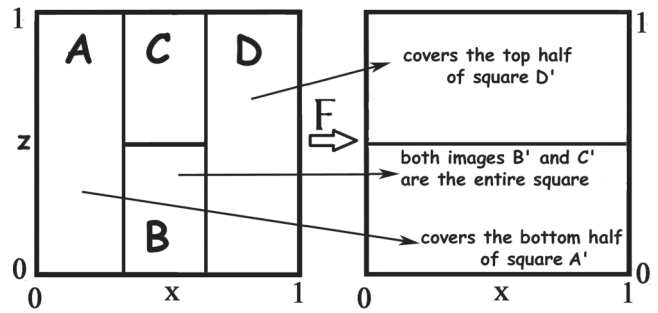


FIG. 2. Our 2D Hetero-chaotic (HC) baker map $B_{HC}(x, z)$. The figure shows a four piece version of the baker map. We divide $0 \leq x < 1$ into three intervals, $L = [0, 1/3)$, $M = [1/3, 2/3)$, and $R = [2/3, 1)$, and divide the square into 3 tall rectangles $A, B \cup C$, and D whose bases are L, M , and R . The map B_{HC} is defined as follows: For $x \in L, z \mapsto z/2$. For $x \in M, z \mapsto 2z \pmod 1$. For $x \in R, z \mapsto z/2 + 1/2$. Then, $x \mapsto 3x \pmod 1$. Hence, B_{HC} expands each rectangle horizontally to full width as shown. The region $\mathcal{R}_1 = A \cup D$ is contracted vertically. The region $\mathcal{R}_2 = B \cup C$ is expanded in both coordinates so that the images of B and C each cover of the entire square. Hence \mathcal{R}_1 and \mathcal{R}_2 are regions of one- and two-dimensional instability.

that has most of its points in \mathcal{R}_1 will have unstable dimension 1 while if most are in \mathcal{R}_2 it has unstable dimension 2.

Unstable Dimension Variability. If a periodic orbit is unstable in k directions, we say it has **UD- k** . In our 2D examples, UD-1 orbits are saddles and UD-2 orbits are repellers. Hence, if an attractor (with a dense trajectory) has a UD-1 orbit and a UD-2 orbit, the attractor has **UDV**.

When an attractor has 2 periodic orbits that are unstable in different numbers of dimensions, we say the attractor has **Unstable Dimension Variability (UDV)**.¹¹

Conjecture 1. Almost every chaotic attractor has the property that if there is one UD- k periodic orbit, then there are infinitely many UD- k periodic points and they lie arbitrarily close to each point of the attractor.

II. HETERO-CHAOS

A set S is a **chaotic attractor** if (1) it is **invariant** (i.e., if a trajectory is in S at some time, then it is in S for all later time), (2) S has a dense trajectory with at least one positive Lyapunov exponent, and (3) trajectories near S are attracted to it as time increases.

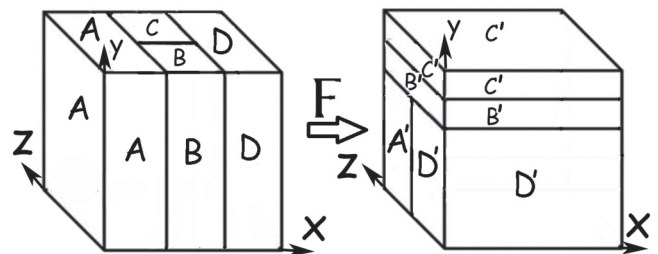


FIG. 3. A volume-preserving 3D version of Fig. 2. Here, the x - z plane plays the role of x - z in Fig. 2 and the y coordinate has been added. Here, the cube is partitioned into four regions A, B, C , and D and for all four $x \mapsto 3x \pmod 1$, and each is mapped into a region of the same volume. We write X' for the image of any region X . Both B and C expand in two directions and contract in one, both having $1/6$ the volume of the cube. A and D each have volume $1/3$ and expand in only the x direction. In other words, the y -height of A' and D' is $2/3$ and the y -height (or thickness) of B' and C' is $1/6$. Note that under F the y coordinate shrinks for all four regions.

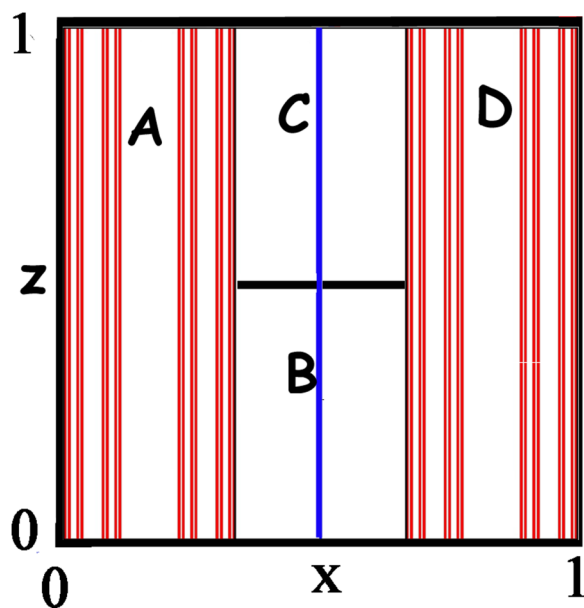


FIG. 4. The invariant “index” sets. For the map in Fig. 2, the vertical red lines here constitute the invariant set whose trajectories stay in \mathcal{R}_1 and the vertical blue line (at $x = 1/2$) is the invariant set of points whose trajectories stay inside \mathcal{R}_2 . In contrast to points on these “index” sets, almost every initial point yields a trajectory that comes arbitrarily close to every point in the square.

We will say a chaotic attractor has **hetero-chaotic** if arbitrarily close to each point of the attractor there are periodic points on UD- k periodic orbits and this is true for multiple values of k . Note that a chaotic “attractor” can have the whole space as is the case with the baker map and our 2D and 3D hetero-chaos baker maps. In Ref. 12, it is called “multi-chaos” but “hetero-chaos” seems more appropriate. We expect that most high-dimensional attractors are hetero-chaotic.

A consequence of UDV is that any trajectory that wanders densely through the invariant set will occasionally get very close to each periodic point. Therefore, that trajectory will spend arbitrarily long intervals of time near each of the fixed points (or periodic orbits). Hence, for each time $T > 0$, the trajectory’s time- T positive Lyapunov exponents will occasionally be the same as for the periodic orbit it approaches.

Conjecture 2. UDV almost always implies hetero-chaos.

Results for the hetero-chaotic baker maps in Figs. 2 and 3. We can prove the maps in Figs. 2 and 3 are hetero-chaotic. Specifically, arbitrarily close to each point q in the square there are periodic points of different UD- k .

Degenerate periodic orbits. It is possible for some periodic orbits to be degenerate. For our 2D HC-baker map, a simple period-2 example has $x = 1/8$ and $3/8$. Then, for each $z \in [0, 1)$, the point $(1/8, z)$ maps to $(3/8, z/2)$ which maps to $(1/8, z)$, so this is periodic. Clearly, there is an infinite collection of such period-2 orbits. There is a corresponding family in the 3D version of the map. More generally, at each iterate of a trajectory, nearby points differing only in the z -coordinate either move apart by a factor of 2 or move closer by a factor of 2, and if a periodic orbit has an equal number of both types, then the orbit is neutrally stable in the z direction. All such

degenerate orbits have even period. Non-degenerate orbits are called **hyperbolic**.

Counting hyperbolic periodic orbits. We can show the numbers of period- N hyperbolic UD-1 and UD-2 periodic orbits are both approximately 3^N when N is large.

Ergodicity. We can show our 2D and 3D HC-baker maps (denoted by F below) are “ergodic” in the following sense. For every continuous function ϕ on the square or the cube, write $\hat{\phi}$ for the average value of ϕ on the cube or the square. The map F is **ergodic** if for almost every initial point q , the trajectory average

$$\frac{1}{N} \sum_{n=1}^N \phi[F^n(q)] \rightarrow \hat{\phi} \text{ as } N \rightarrow \infty.$$

Due to the ergodicity, we can also conclude that there is a dense trajectory. In fact, ergodicity for our baker maps implies that for almost every initial point q , the trajectory $F^n(q)$ for $n \geq 0$ comes arbitrarily close to every point of the square or cube, respectively.

The proofs of the statements that F is hetero-chaotic and ergodic will be provided elsewhere.

The route to hetero-chaos when the attractor changes continuously with a parameter. In addition to presenting low-dimensional examples, the purpose of this paper is to ask how hetero-chaos arises from homogeneous chaos as some physical parameter is varied. We show numerical evidence that the Zigzag map in Fig. 5 (where $\sigma = 5$) is homogeneously chaotic for $\alpha < \alpha_{HC} \sim 0.31$ and is hetero-chaotic for $\alpha > \alpha_{HC}$. Similarly, we show numerical evidence that the Kostelich map (Eq. 1) is homogeneously chaotic for $\sigma < \sigma_{HC} = 1/\pi \sim 0.318$ and appears to be hetero-chaotic for $\sigma > \sigma_{HC}$, when $\alpha = 0.07$.

We believe if an attractor is changing continuously, the transition will occur at a periodic orbit bifurcation and we give some examples of this transition.

The crisis route to hetero-chaos. As some parameter, say α , is varied, a “crisis” occurs at some value α_0 when there is a sudden discontinuous change in the size of a chaotic attractor. Hence, a crisis can be seen as a sudden jump in the plot of an attractor versus α . On the side of α_0 where the attractor is small, the attractor could be homogeneously chaotic. On the other side, the attractor can be much larger and can include periodic orbits of a different UD value. Then the attractor has UDV and appears to be hetero-chaotic. See Refs. 12–15.

The continuous route to hetero-chaos. If as a parameter α is varied, a homogeneous chaotic attractor suddenly becomes hetero-chaotic after some $\alpha = \alpha_{HC}$, we say a **hetero-chaos bifurcation (HCB)** occurs at α_{HC} . What is the nature of this bifurcation? As a parameter changes, a periodic orbit in a chaotic attractor can migrate to a region that is more unstable, and the orbit’s UD value can increase. Then, an exponent of that orbit will pass through 0 and a bifurcation will occur. Or a new pair of orbits can appear in an analogue of a saddle-repeller bifurcation, with UD values k and $k + 1$ for some $k > 0$.

Conjecture 3. For a typical attractor, if an HCB occurs as the attractor changes continuously (without a crisis), then

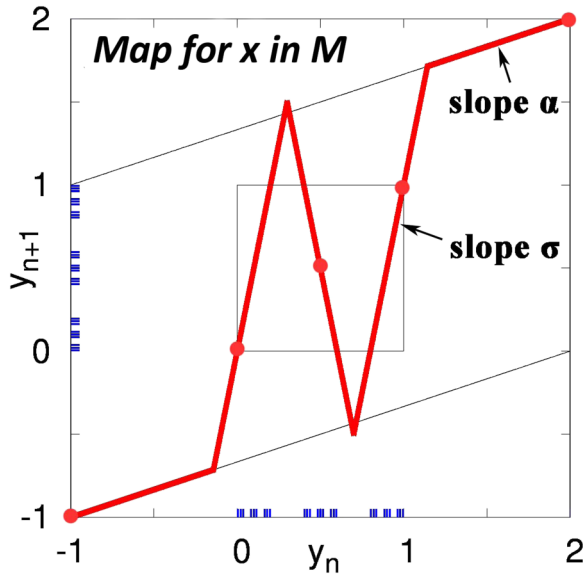


FIG. 5. Defining our Zigzag map. Here, as in Fig. 2, the definition of the map depends on which of the three intervals x is in: $L = [0, 1/3)$, $M = [1/3, 2/3)$, and $R = [2/3, 1)$. For $x \in L$, $y \mapsto -1 + \alpha(y + 1)$. For $x \in R$, $y \mapsto 2 + \alpha(y - 2)$. For $x \in M$, the figure shows the map. Each of the three maps is from $[-1, 2]$ into itself. The horizontal coordinate $x \mapsto 3x \bmod 1$. Each slope in the map shown is either $0 < \alpha < 1$ or $\pm\sigma$, where $\sigma > 3$. Here $\alpha = 1/3$, and $\sigma = 5$ both here and in Fig. 6. All 5 fixed points are shown with large red dots. The Zigzag map has an invariant fractal set on the vertical line for which $x = 1/2$ (x is not shown). Here, these y values are illustrated using dots on axes.

there will be a periodic orbit bifurcation, i.e., either period-doubling or pitchfork or Hopf or pair-creation such as saddle-repeller.

Expanding regions \mathcal{R}_k and “index sets.” Let \mathcal{R}_k denote the region of phase space in which the dynamics (specifically, the map’s Jacobian) is k -dimensionally expanding; see e.g., Fig. 2. We call the largest invariant set that lies wholly in \mathcal{R}_k the **index- k set**. In Fig. 2, \mathcal{R}_1 and \mathcal{R}_2 are described. The index sets for the 2D HC baker map are shown in Fig. 4.

At the center of Fig. 6-Right for the Zigzag map (Fig. 5), there is a different \mathcal{R}_2 , the white rectangle ($1/3 < x < 2/3$,

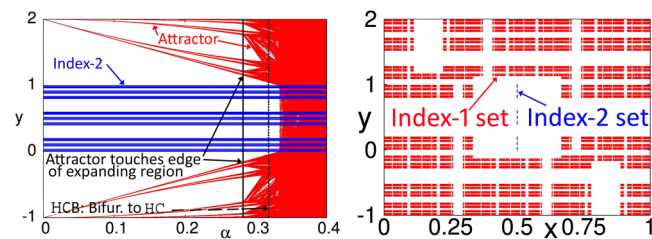


FIG. 6. The Zigzag map’s bifurcation diagram and index sets. Left panel. The chaotic attractor (red) is shown increasing in size as α increases. The blue set is the index-2 set. At $\alpha \approx 0.28$ (solid black vertical line), the attractor begins to move into the expanding region, but the attractor does not contain repelling periodic points until after $\alpha_{HC} \approx 0.31$ (dotted black vertical line), when a period-4 repeller exists. Then, there is hetero-chaos. At $\alpha = 1/3$, there is a “crisis” after which the attractor jumps in size and is the entire x - y square. Right panel. Here $\alpha = 0.4 (> 1/3)$. We show only the index-1 set (red) and the index-2 set (blue), which is on the vertical line $x = 1/2$. This illustrates that within the hetero-chaotic attractor (the entire square) there are relatively large index sets.

$-c < y < 1 + c$), where $c = (1 - \alpha)/(\sigma - \alpha) \approx 0.13$, and \mathcal{R}_1 is the rest, excluding boundary points.

It probably seems strange that the existence of two periodic orbits with different UD values has such a dramatic consequence for an attractor that it implies hetero-chaos. Our response is that these orbits generally lie in index sets, that can be quite big as Figs. 2 and 6 illustrate.

III. HETERO-CHAOS CONNECTS MANY PHENOMENA LIKE FLUCTUATING EXPONENTS (FE) AND UDV

Hetero-chaotic attractors contain periodic orbits with different UD values. A typical trajectory will return near each, occasionally spending long times near them before moving on, and while near the periodic orbit of a region, it will have the same number of positive finite-time Lyapunov exponents (FTLEs) as the periodic orbit. As it moves among the periodic orbits, its number of positive FTLEs fluctuates (for each time $T > 0$); see Refs. 16 and 17. This property is referred to as FE (Fluctuating Exponents). Some papers have used the term UDV to mean FE. UDV and FE are both implied by other dynamical phenomena in the literature such as riddled basins, blowout bifurcations, on-off intermittency, and chaotic itinerancy.^{18–22}

Transitions from homogeneous chaos to FE or UDV have been observed in Refs. 17, 23, and 24, but the mechanism of the transitions is not discussed.

Shadowing. It is important for a physicist to know how good a numerical simulation is—as in a climate simulation—and for how long it is valid. When each numerical trajectory stays close to some actual trajectory of the system, we say the system has the **shadowing property**, i.e., simulations are realistic.

When a trajectory moves from a region where the dynamics has fewer unstable directions to a region where it has more, shadowing fails, and trajectories become unrealistic—see Fig. 3 of Ref. 25. Such a transition causes fluctuations in the number of positive FTLEs, which means FE will be common in higher-dimensional attractors.

The FE property implies shadowing fails, as was established by Dawson *et al.*¹⁶ Homogeneous chaotic systems can have the shadowing property but hetero-chaotic systems cannot, as shown for UDV in Refs. 25–27.

Hetero-chaos is not Hyper-chaos. Hetero-chaos should not be confused with “hyper-chaos.”^{28,29} A hetero-chaotic attractor can have one or more positive Lyapunov exponents. It need not be hyper-chaotic (i.e., have more than one positive Lyapunov exponent). Furthermore, all periodic orbits of a hyper-chaotic attractor might have the same UD value, in which case it would not be hetero-chaotic.

UDV in the mathematics literature. The first examples of a (robust) invariant set containing periodic orbits with different UD values were given by Abraham and Smale³⁰ and Simon³¹ in four and three dimensions, respectively. “Robust” means the property persists under all sufficiently small perturbations. Later, it was mathematically studied using the notions of “blenders” and “hetero-dimensional cycles” (see Ref. 32 and references therein). That literature generally shows no

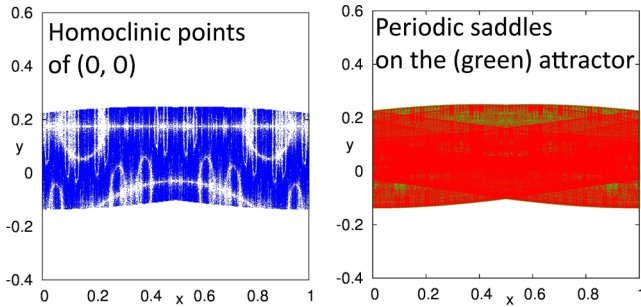


FIG. 7. Homoclinic points and periodic saddles for Kostelich map. It can be shown that both saddles and repellers are dense in the attractor, so that we have hetero-chaos. This figure shows what the sets of homoclinic points and periodic points look like for limited computations. Left panel. Points in the attractor that map to the repelling origin within 14 iterates. Since they are in the unstable manifold of $(0, 0)$, they are homoclinic points. In fact, the homoclinic points can be shown to be densely distributed in the attractor implying that repelling periodic points are dense, since Marotto³⁴ shows that arbitrarily close to each homoclinic point there are repelling periodic points. Right panel. The saddle periodic points (red) of period 13 are plotted on top of the chaotic attractor (green). They become denser as the period increases.

interest in whether their invariant sets are (physically observable) attractors.

IV. TWO MORE HETERO-CHAOTIC MAPS

Our “Zigzag” map and its route to hetero-chaos. As with the 2D HC Baker Map, the next 2D map has x dynamics described by $x \mapsto 3x \bmod 1$, and its y dynamics depends on whether x is in L , M , or R . It has two slope parameters, α and σ . Figure 5 shows the y dynamics on M and the caption gives the map also on L and R . The map has an index-2 fractal invariant set on the vertical line at $x = 1/2$ for every α and every $\sigma > 1$; (we use $\sigma = 5$ and then its dimension is

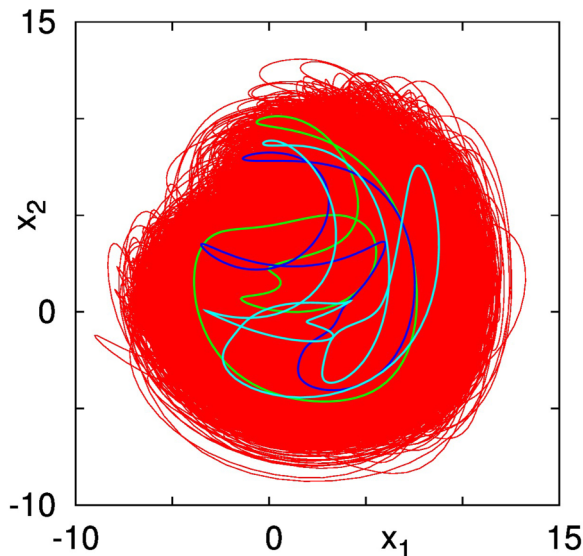


FIG. 8. A projection of the chaotic attractor and three periodic orbits with different UD values. This shows a projection into the x_1 - x_2 plane of orbits O_1 , O_2 , and O_3 with UD-1 (green), 2 (blue), and 3 (light blue), respectively. There are infinitely many possible projections of \mathbb{R}^8 into a plane and all those tested show all three periodic orbits lying within the projected attractor. See also Fig. 9.

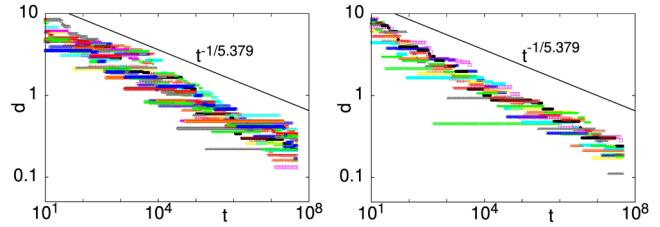


FIG. 9. Trajectories approach 3 periodic orbits. We investigated three periodic orbits O_1 , O_2 , and O_3 in Fig. 8, O_1 in the left panel and O_2 in the right. The graph for O_3 is omitted since it is quite similar to the right panel. We chose 21 initial conditions very close to each other. In each panel, for each of 21 trajectories, the closest approach by time t to the respective periodic orbit is reported. The 8 Lyapunov exponents for the global chaotic attractor are as follows: 1.594, 0.390, 0.0, -0.453 , -0.960 , -1.508 , -2.450 , -4.613 . A standard estimate of a dimension of a chaotic attractor is its “Lyapunov” dimension.³⁸ The Lyapunov dimension of the attractor is 5.379 and according to a long-standing conjecture, Farmer *et al.*⁹ the closest approach of a typical trajectory to a typical point of the attractor is expected to be proportional to $t^{-1/5.379}$ for time $t \in [0, t]$. The straight line indicates that rate of closest approach to that orbit (though periodic orbit points are not generally typical). The straight line has been shifted vertically slightly. For all three, the actual convergence appears slightly faster than expected. It suggests that given sufficient time the typical trajectory would come arbitrarily close to all three periodic orbits. The Lyapunov dimension for these periodic orbits are 5.268 for O_1 , 5.107 for O_2 , and 5.514 for O_3 .

$\ln 3/\ln 5 \approx 0.683$). The attractor is chaotic for all $\alpha > 0$, and for $\alpha < 0.28$ is an index-1 set.

As α increases from 0, at $\alpha_{HC} \approx 0.31$ (see the left panel of Fig. 6), there is a pitchfork bifurcation of a period-4 periodic orbit, one of whose branches consists of repellers. Numerically, this appears to be the first occurrence in the attractor of a repelling periodic orbit. This observation supports Conjecture 3. Hence, the HCB occurs at α_{HC} .

At $\alpha = 1/3$, the attractor collides with the index-2 set, after which the attractor suddenly jumps in size, covering the whole x - y square. For $\alpha = 0.4$, the attractor is the whole torus and both index-1 and index-2 sets coexist (see the right panel of Fig. 6). We have identified the index sets by using the Stagger-and-Step method.³³

Kostelich map. The following smooth map^{11,12} is defined on a two-dimensional torus:

$$\begin{aligned} x_{n+1} &= 3x_n \bmod 1 \\ y_{n+1} &= y_n - \sigma \sin(2\pi y_n) + \alpha[1 - \cos(2\pi x_n)] \bmod 1. \end{aligned} \quad (1)$$

It has an HCB whose periodic orbit bifurcation is a period-doubling at the origin, a fixed point that becomes a repeller. We find numerically that immediately after the bifurcation, the chaotic attractor has a dense set of repellers and a dense set of saddles. This observation also supports Conjecture 3. For $\alpha = 0.07$ and $\sigma \in (0.2, 1/\pi)$, there is a chaotic attractor for which all periodic orbits in the attractor are saddles. The origin period-doubles as σ increases at $\sigma = \sigma_0 = 1/\pi \sim 0.318$ (the HCB value). As σ increases from beyond σ_0 a new index-2 set appears in the attractor, and repelling periodic orbits are immediately dense in the attractor (Fig. 7, left, for $\sigma = 0.35$), and the saddle periodic orbits are still dense in the attractor (Fig. 7, right).

Lower-triangular Jacobians. Our hetero-chaotic baker maps and the maps in this section have the following property. Each periodic orbit lying wholly in some \mathcal{R}_k has UD- k . This is

true because for each map F , the Jacobian matrix $DF(x, y)$ is lower triangular. Such maps are called “skew products.” The Jacobian DF^T of the time- T map F^T is also lower triangular since by the chain rule, DF^T is the product of T of these matrices DF . The number of expanding directions for a point is the number of diagonal elements of DF that are > 1 .

V. LORENZ-96 MODEL

So far in this paper, we have considered maps rather than differential equations in order to keep the models as simple as possible, but our real goal is to understand higher dimensional hetero-chaotic differential equations. Edward Lorenz proposed a variety of closely related chaotic differential equation models. See Ref. 35 for connections among them and for some generalizations. In particular, Lorenz^{36,37} proposed a dissipative N -dimensional ODE as a model of some oscillating scalar atmospheric quantity described by

$$\frac{dx_k}{dt} = x_{k-1}(x_{k+1} - x_{k-2}) - x_k + f, \quad \text{for } k = 1, \dots, N,$$

where the system has cyclical symmetry, so $x_{N+k} = x_k$ for all $k = 1, \dots, N$, and where f is a forcing parameter. We use the case $N = 8$. For the Lorenz-96 model with $f = 8$, the chaotic attractor has Lyapunov dimension 5.379. Numerically, we found many periodic orbits of UD-1, 2, and 3, and no periodic orbits with UD- k ($k > 3$). Three of them with different UD values are shown in Fig. 8. The distances between three periodic orbits and chaotic orbits were calculated and shown in Fig. 9. This implies that the periodic orbits are in the attractor and the attractor has UDV, and at least according to our conjecture it is also hetero-chaotic.

VI. DISCUSSION

We began this project to try to understand how such a phenomenon as hetero-chaos could exist with trajectories wandering through very different kinds of regions. We believe hetero-chaos is important for all models with high-dimensional attractors including weather prediction and climate modeling. It is perhaps the unifying concept linking different phenomena observed in numerous numerical simulations of chaotic dynamical systems and physical experiments, such as unstable dimension variability (UDV), on-off intermittency, riddled basins, blowout, and bubbling bifurcations. It is also a major cause of shadowing to fail, i.e., for simulated solutions to be non-physical. We have made three conjectures as the beginning of a general theory of hetero-chaos.

Hetero-chaotic systems have been particularly difficult to visualize, so we have introduced some low-dimensional examples as paradigms, including our baker maps that are perhaps the simplest possible examples of hetero-chaos. See Figs. 2 and 3.

Our baker maps are only the second example(s) proved to have a hetero-chaotic attractor. (We think of our 2D and 3D examples as different aspects of a single example.) The first case¹² had a quasi-periodic set in the attractor. Yet quasi-periodicity would appear to have little to do with hetero-chaos. So our examples here (which do not have quasi-periodicity) is reassuring and much simpler.

We investigate how hetero-chaos arises as a parameter is varied. It can either occur at a crisis, that is a sudden jump in the size of the chaotic attractor, or it can occur when the attractor is changing continuously. In the latter case, we find that the transition to hetero-chaos occurs at a periodic orbit bifurcation, and we believe this is the typical case when the attractor varies continuously. Because shadowing fails for hetero-chaotic systems, detecting the transition from homogeneous chaos to hetero-chaos can be critical for prediction efforts.

While the UDV condition requires only two orbits of different UD values, we have focused on the existence of not just these two orbits but much larger index sets which exist in hetero-chaotic attractors and make hetero-chaos persistent.

Because of the increasing importance of models with high dimensional chaotic attractors, we have tried to create terminology that is easy to use.

ACKNOWLEDGMENTS

Y.S. was supported by the JSPS KAKENHI Grant No. 17K05360 and JST PRESTO No. JPMJPR16E5. M.A.F.S. was supported by the Spanish State Research Agency (AEI) and the European Regional Development Fund (FEDER) No. FIS2016-76883-P and jointly by the Fulbright Program and the Spanish Ministry of Education No. FMECD-ST-2016.

¹E. Pariat, J. E. Leake, G. Valori, M. G. Linton, F. P. Zuccarello, and K. Dalmasse, *Astron. Astrophys.* **601**, A125 (2017).

²F. Guzzetti, *Toxicol. Environ. Chem.* **98**, 1043 (2016).

³K. Tian, N. N. Gosvami, D. L. Goldsby, Y. Liu, I. Szlufarska, and R. W. Carpick, *Phys. Rev. Lett.* **118**, 076103 (2017).

⁴D. J. Patil, B. R. Hunt, E. Kalnay, J. A. Yorke, and E. Ott, *Phys. Rev. Lett.* **86**, 5878 (2001).

⁵A. S. Gritsun, *Russ. J. Numer. Anal. Math. Model.* **23**, 345 (2008).

⁶A. S. Gritsun, *Phil. Trans. R. Soc. A* **371**, 20120336 (2013).

⁷W. Seidel, *Proc. Natl. Acad. Sci. U.S.A.* **19**, 453 (1933).

⁸P. R. Halmos, *Lectures on Ergodic Theory* (Chelsea Publishing Company, New York, NY, 1956), p. 9.

⁹J. Farmer, E. Ott, and J. Yorke, *Physica D* **7**, 153 (1983).

¹⁰J. C. Alexander and J. A. Yorke, *Ergodic Theory Dyn. Syst.* **4**, 1 (1984).

¹¹E. J. Kostelich, I. Kan, C. Grebogi, E. Ott, and J. A. Yorke, *Physica D* **109**, 81 (1997).

¹²S. Das and J. A. Yorke, *SIAM J. Appl. Dyn.* **16**, 2196 (2017).

¹³K. T. Alligood, E. Sander, and J. A. Yorke, *Phys. Rev. Lett.* **96**, 244103 (2006).

¹⁴R. Viana, C. Grebogi, S. de S. Pinto, S. L. A. Batista, and J. Kurths, *Physica D* **206**, 94 (2005).

¹⁵R. F. Pereira, S. E. de S. Pinto, R. L. Viana, S. R. Lopes, and C. Grebogi, *Chaos* **17**, 023131 (2007).

¹⁶S. P. Dawson, C. Grebogi, T. Sauer, and J. A. Yorke, *Phys. Rev. Lett.* **73**, 1927 (1994).

¹⁷S. P. Dawson, *Phys. Rev. Lett.* **76**, 4348 (1996).

¹⁸E. Ott, J. C. Sommerer, J. C. Alexander, I. Kan, and J. A. Yorke, *Phys. Rev. Lett.* **71**, 4134 (1993).

¹⁹N. Platt, E. A. Spiegel, and C. Tresser, *Phys. Rev. Lett.* **70**, 279 (1993).

²⁰J. F. Heagy, N. Platt, and S. M. Hammel, *Phys. Rev. E* **49**, 1140 (1994).

²¹E. Ott and J. C. Sommerer, *Phys. Lett. A* **188**, 39 (1994).

²²I. Tsuda, *Chaos* **19**, 015113 (2009).

²³P. Moresco and S. P. Dawson, *Phys. Rev. E* **55**, 5350 (1997).

²⁴E. Barreto and P. So, *Phys. Rev. Lett.* **85**, 2490 (2000).

²⁵C. Grebogi, L. Poon, T. Sauer, J. A. Yorke, and D. Auerbach, in *Handbook of Dynamical Systems*, edited by B. Fiedler (North-Holland, Amsterdam, 2002), Vol. 2, pp. 313–344.

²⁶T. Sauer, C. Grebogi, and J. A. Yorke, *Phys. Rev. Lett.* **79**, 59 (1997).

²⁷G. C. Yuan and J. Yorke, *Proc. Am. Math. Soc.* **128**, 909 (2000).

²⁸O. E. Rössler, *Phys. Lett. A* **71**, 155 (1979).

²⁹M. A. Harrison and Y.-C. Lai, *Int. J. Bifurcat. Chaos* **10**, 1471 (2000).

- ³⁰R. Abraham and S. Smale, in *Global Analysis (Proceedings of Symposia in Pure Mathematics, Vol. XIV, Berkeley, CA, 1968)* (American Mathematical Society, Providence, RI, 1970), pp. 5–8.
- ³¹C. P. Simon, *Proc. Am. Math. Soc.* **34**, 629 (1972).
- ³²C. Bonatti, L. Díaz, and M. Viana, *Dynamics Beyond Uniform Hyperbolicity* (Springer-Verlag, Berlin, 2005).
- ³³D. Sweet, H. E. Nusse, and J. A. Yorke, *Phys. Rev. Lett.* **86**, 2261 (2001).
- ³⁴F. R. Marotto, *Chaos Solitons Fractals* **25**, 25 (2005).
- ³⁵Y. Saiki, E. Sander, and J. Yorke, *Eur. Phys. J. Spec. Top.* **226**, 1751 (2017).
- ³⁶E. Lorenz, in *Seminar on Predictability* (ECMWF, Reading, 1996), Vol. 1, pp. 1–18.
- ³⁷E. Lorenz and K. Emanuel, *J. Atmos. Sci.* **45**, 399 (1998).
- ³⁸K. Alligood, T. Sauer, and J. Yorke, *Chaos An Introduction to Dynamical Systems* (Springer-Verlag, New York, NY, 1996).